Annales Geophysicae (2002) 20: 1857–1862

Annales Geophysicae

On the influence of neutral turbulence on ambipolar diffusivities deduced from meteor trail expansion

C. M. Hall

Tromsø Geophysical Observatory, Tromsø, Norway

Received: 13 September 2001 – Revised: 15 April 2002 – Accepted: 17 April 2002

Abstract. By measuring fading times of radar echoes from underdense meteor trails, it is possible to deduce the ambipolar diffusivities of the ions responsible for these radar echoes. It could be anticipated that these diffusivities increase monotonically with height akin to neutral viscosity. In practice, this is not always the case. Here, we investigate the capability of neutral turbulence to affect the meteor trail diffusion rate.

Key words. Meteorology and atmospheric dynamics (middle atmosphere dynamics; turbulence)

1 Introduction

Meteors entering the Earth's atmosphere generate trails of ionized gas that optimised radars can utilize to obtain information about winds and temperatures (Tsutsumi et al., 1999). In order to determine the latter, echo fading, assumed to be a consequence of ambipolar diffusion of the ions constituting the meteor trail, is measured whenever the plasma frequency is less than the radar frequency (known as "underdense" echoes). The process of deriving temperatures from the measurements of an ambipolar diffusion coefficient are fraught with uncertainty (e.g. Jones, 1995), although at the peak of echo occurrence, many satisfactory results have been obtained (e.g. Hocking, 1999). To make matters worse, however, the measured ambipolar diffusivities themselves may be unreliable, as predicted by Dyrud et al. (2001). The diffusivity of air increases exponentially with height, and one would expect the ambipolar diffusivity of the meteor-trail ions to behave similarly. In practice, however, meteor radars often yield profiles that are almost constant with altitude below 90 km and actually decrease with height in the lower thermosphere. Since echoes are largely obtained from a height regime only a few kilometers wide, centered on around 90 km, for a radar operating at, say, 30 MHz, statistics in the lower thermosphere and mid-mesosphere are poor and, thus, the results are more susceptible to noise. In these profiles, the shape tends towards height independence in the lowest parts while exhibiting a sudden decrease with altitude in the upper part, hence, a "7" form. Despite the noise on either side of the peak occurrence height, the "figure seven" shaped profiles occur so frequently that they deserve investigation. Here, we will address the height independent nature of the lower part of the diffusivity profile. The upper part of the profile is thought to be a consequence of the degree to which the observed echo fading is a mixture of diffusion along and perpendicular to the magnetic field (Dyrud et al., 2001).

Correspondence to: C. M. Hall (chris.hall@tgo.uit.no)

2 Simulation of ambipolar diffusivity profiles

Although the phenomena described above apply to many radar results (Hocking, private communication), we shall consider a high latitude case: 80° N, this corresponding to the newly installed Nippon / Norway Svalbard Meteor Radar (NSMR) (Aso et al., 2001). We employ the MSISE90 model atmosphere of Hedin (1991) to obtain neutral density and temperature, T, profiles and, therefore, atmospheric pressure, P. Hence, the ambipolar diffusivity D_a of ions is given by:

$$D_a = \frac{k_B T}{e} \cdot \frac{T}{T_0} \cdot \frac{P_0}{P} \cdot K_0 \cdot \left(1 + \frac{T_e}{T_i}\right) , \quad (1)$$

where k_B is Boltzmann's constant, T_0 = 273.16 K and P_0 = 1.013×10^5 Pa are standard temperature and pressure, respectively, K_0 is the zero-field reduced mobility of the ions, e is the electronic charge, and T_e and T_i are the electron and ion temperatures, respectively, in the plasma (e.g. Chilson et al., 1996). Since collisions are frequent at the altitudes in question (we shall consider below 90 km), the electron, ion and neutral gas temperatures will be considered equal. The mobility, K_0, depends on the ion species. Hence, assuming, for example, ions with mass number of 40, which corresponds to a combination of Mg^+ and Fe^+ giving K_0 = $2.5 \times 10^{-4}\,m^2V^{-1}\,s^{-1}$, we can model the ambipolar diffusion

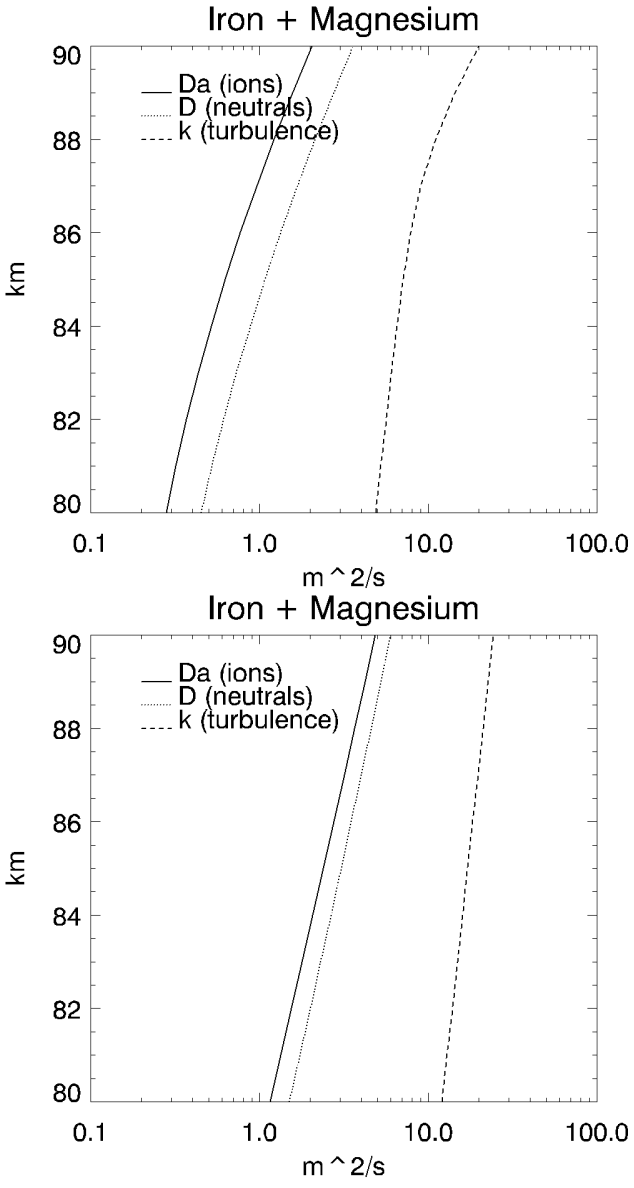

Fig. 1. Diffusion coefficient profiles. Solid lines: ambipolar diffusion assuming a mixture of Fe^+ and Mg^+; Dotted lines: neutral atmosphere; Dashed line: turbulence (see text). Upper panel: summer; lower panel: winter.

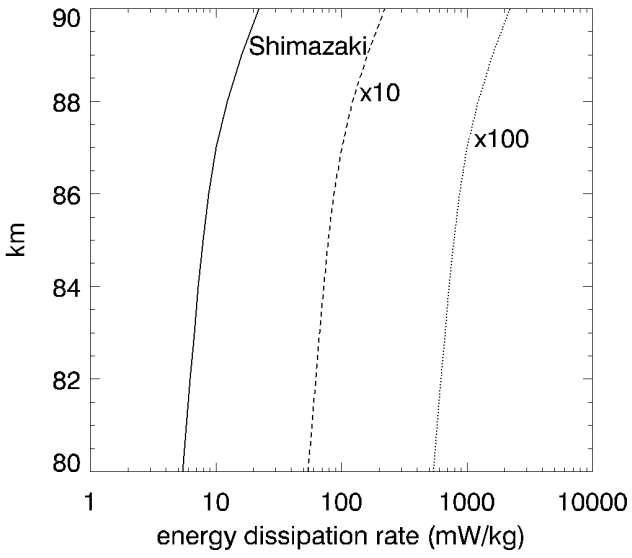

Fig. 2. Modelled (see text) turbulent energy dissipation rates. Solid line: Shimazaki (1971) shape normalized to Danilov and Kalgin (1996); Dashed line: moderate turbulence scenario (solid line × 10); Dotted line: strong turbulence scenario (solid line × 100).

coefficient profile. Similarly, it is a straightforward matter to model the corresponding neutral gas diffusivity D (or kinematic viscosity). The turbulent diffusivity K may also be modelled (Hall et al., 1998) by normalizing the model of Shimazaki (1971) to the measurements of Danilov and Kalgin (1996). This is a particularly pertinent approach in this case, since the latters' observations were from Heiss Island, also at approximately 80° N. While details are to be found in Hall et al. (1998), the essence of the model is that maxima in K and their altitudes are obtained from Danilov and Kalgin (1996) as a function of season, and these are used to fix the corresponding points in the profile shape supplied by Shimazaki (1971). The resulting profiles, derived for mid-summer and for mid-winter at 80° N are shown in Fig. 1. Changing the ion species to N_2^+ results in a half magnitude reduction in D_a, not shown here. We see an overall increase in diffusivity levels from summer to winter, but most pronounced for D and D_a.

Turbulence tends to occur in layers and intermittently. Therefore, at any one time we would expect to see a profile of turbulent intensity exhibiting much more structure than suggested by Fig. 1. More importantly, one would expect temporally and spatially localized instances of considerably stronger turbulence than indicated by the model. On occasion, up to 2 orders of magnitude greater intensity could occur and likewise instances of little or no turbulence at all. Converting the model profile for summer only into an equivalent energy dissipation rate, ϵ, using Weinstock (1978):

$$\epsilon = K\omega_B^2/0.81 \,, \tag{2}$$

in which ω_B is the Brunt Väisälä frequency (derivable from MSISE90), we can obtain an idea of the magnitudes of turbulent intensities in the height regime of interest here (Fig. 2).

The time scale, τ, associated with the dissipative nature of turbulence, may be defined as (Tennekes and Lumley, 1972):

$$\tau = (\upsilon/\epsilon)^{1/2} \,, \tag{3}$$

where υ is the kinematic viscosity. This kinematic viscosity, or alternatively momentum diffusivity (e.g. Batchelor, 1970) is usually considered identical to the mass diffusivity (e.g. Hinze, 1975), i.e. half of the value of the ambipolar diffusivity, of the fluid into which turbulence is dissipating kinetic energy, and in this case, we shall assume it is into the plasma, which, in turn, is in thermal equilibrium with the air. In any case, the diffusivities of air and plasma, particularly

if the primary ion is N_2^+, are very similar. Thus, we are able to model turbulence time scales for the summer and winter cases, for each of the turbulence intensity scenarios, and for each of the suggested ion species. The reader is referred to Batchelor (1970), Hinze (1975) and Kundu (1990) for more information on turbulent and molecular diffusivities of momentum mass and heat, and the Schmidt (Sc) and Prandtl numbers parameterising the relationships between them.

After a meteor passes through the atmosphere, the resulting ionized column expands very rapidly (within a millisecond or so) until thermal equilibrium is reached, at which point the trail is said to have an "initial radius". When this initial radius is short compared with the quarter radar wavelength, scattering from within the trail is coherent. Eventually, as the radius expands and becomes much larger than the radar wavelength, the scattering becomes incoherent and invisible to classic meteor radar systems (McKinley, 1961). Considering now the time during which the trail delivers coherent echoes, the time evolution of the echo amplitude $A(t)$ is given by McDaniel and Mason (1973):

$$A(t) = A_0 \exp\left(-16\pi^2 D_a t/\lambda^2\right) , \quad (4)$$

where A_0 is the initial value of the echo amplitude and λ is the radar wavelength. For the case of NSMR, operating at 31 MHz, the wavelength is 9.67 m. During this evolution, the length scales of any ambient neutral turbulence (eddy sizes, for convenience) should be comparable with the radar wavelength, in order to be able to help destroy the echo coherency and, therefore, enhance the echo fading. The length scales η, the Kolomorov microscale, corresponding to the time scales given in Eq. (3) for the ϵ shown in Fig. 2, are illustrated in Fig. 3 (Kolmogorov, 1941; Tennekes and Lumley, 1972), with η being obtained from

$$\eta = \left(\nu^3/\epsilon\right)^{1/4} . \quad (5)$$

In Fig. 3, the kinematic viscosity is that of the ambient atmosphere (Hedin 1991), with the neutral eddies being assumed to transport the meteor trail plasma and $Sc = 1$, since ϵ here is a metric for the neutral turbulence. The length scale η is the scale at which the extrapolations of the slopes of viscous and inertial regimes of the turbulent spectrum meet. An alternative is to consider the length scale at which the inertial subrange begins to depart from a power-law dependence; this scale, the inner scale l_0, is typically given by 7.4η (Blix et al., 1990), this perhaps better representing the smallest eddies, and is also shown in Fig. 3. We see, therefore, that the above condition is met: these length scales correspond (roughly speaking) to the smallest eddies and so we see that, at least at 80 km, for a radar wavelength of around 10 m, eddies exist for only slightly enhanced turbulence. (The concept of eddies is used here for convenience only and for a more correct description of turbulence, the reader is referred to the references given).

Modelled echoes based on Eq. (4) are shown in Fig. 4 (metal ions) and Fig. 5 (nitrogen); the upper panels show

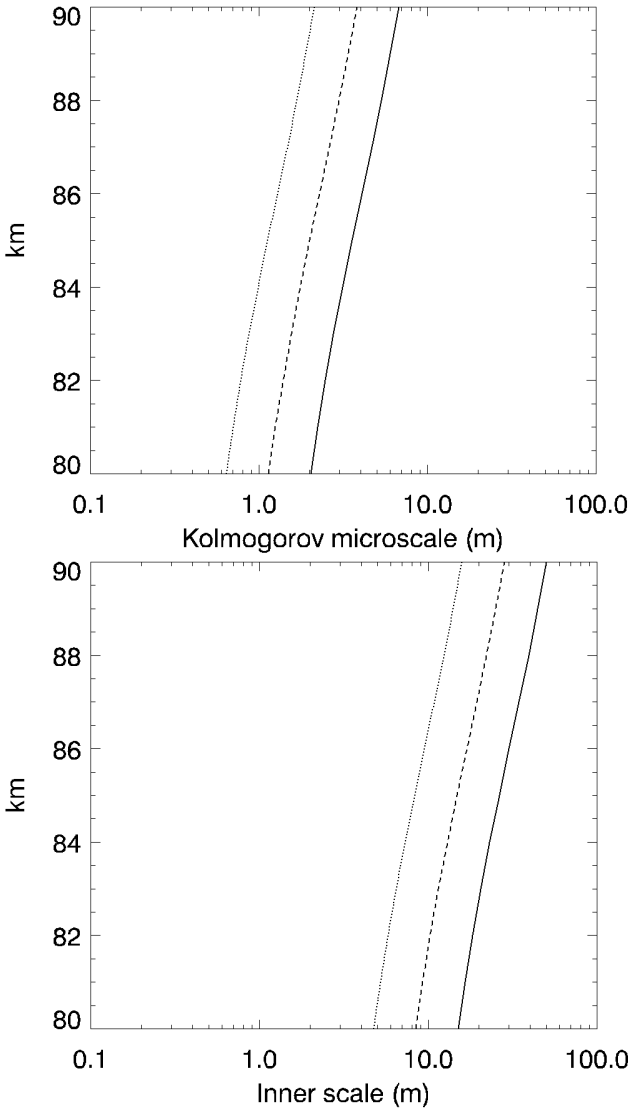

Fig. 3. Length scales (Kolmogorov microscale η and inner scale l_0) profiles for summer and corresponding to the modelled energy dissipation rates portrayed in Fig. 2. The strong turbulence scenario is the leftmost profile in each case.

summer cases and the lower winter. We see that with increasing levels of turbulent intensity, parameterized by a decreasing characteristic time scale, turbulent mixing can begin to dominate the dissipation of the meteor trail. To take an example, consider summer at 80 km and when turbulence is strong: in the case of metallic ions forming the meteor trail, turbulence will start to take over as the dissipation mechanism after only 0.5 s. If the time to which echo amplitude falls to 1/e of its initial value is determined and used as a basis for estimating D_a using Eq. (4), D_a will be overestimated, since the echo amplitude will decrease more rapidly with time after it has fallen to 0.6 of its initial value. If a linear fit of $A(t)$ is performed in logarithmic space, the resulting (negative) slope will be steeper and again, D_a will be overestimated. Thus, even though the turbulent time scale may be

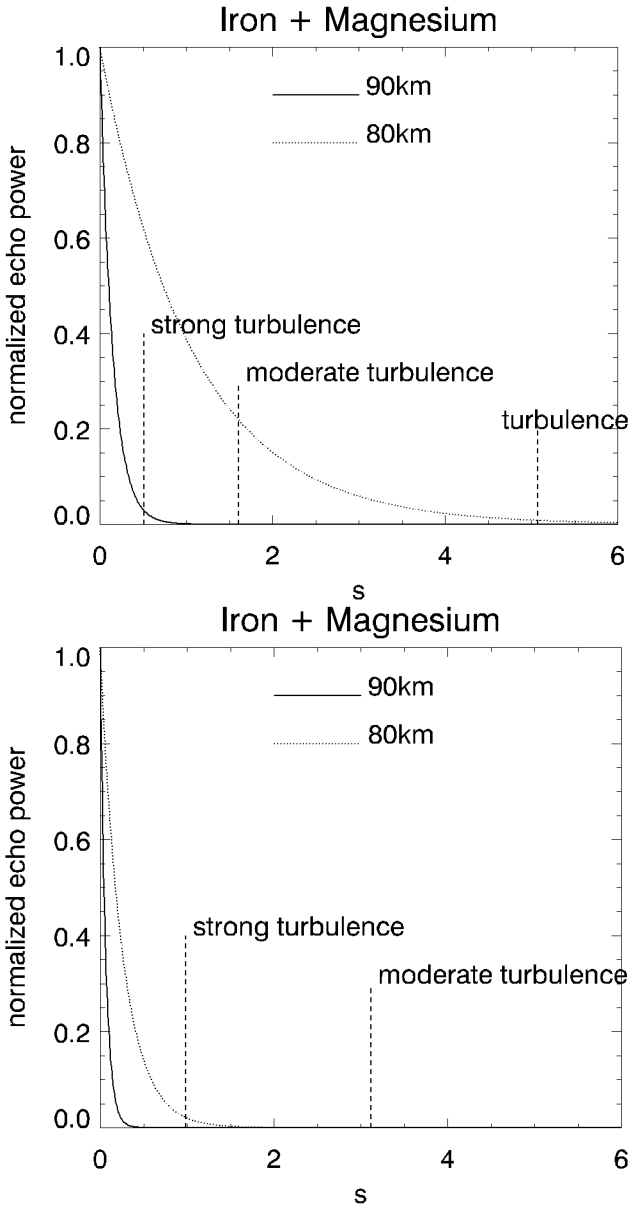

Fig. 4. Simulated meteor trail echoes assuming metal ions. Upper panel: summer; Lower panel: winter. Two heights are shown, 80 and 90 km (dotted and solid lines, respectively). The time scales corresponding to "average", "moderate" and "strong" turbulence are shown by the vertical dashed line segments.

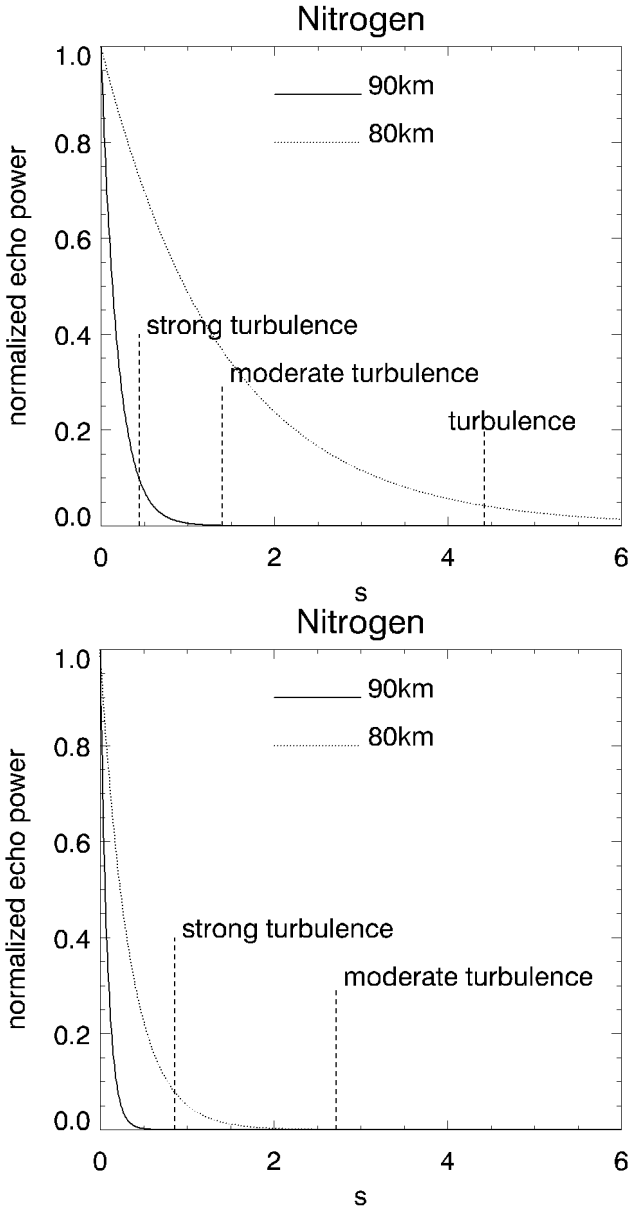

Fig. 5. As for Fig. 4, but for nitrogen.

greater than the time taken for the amplitude to drop to, say, 1/2 or 1/e of its initial value, the derived ambipolar diffusivity may be affected, depending on the analysis technique. Furthermore, recall that the echo decay time is proportional to the square of the radar wavelength squared. So for lower frequencies, the echo will be more persistent and the problem will be more acute. Although the simulations shown here indicate little difficulty at 90 km altitude, turbulent diffusivity is relatively constant with height up to the turbopause (at which there is an abrupt cutoff, the very definition of the turbopause). Thus, for a meteor observation using an MF (e.g. 3 MHz) radar, turbulence could present a problem at higher altitudes (W. Hocking, private communication).

Finally, taking the strong turbulence case and assuming that the characteristic echo fading time is defined by the time taken for the amplitude to fall to one-half of its initial value (just one possible approach, so solving Eq. 4) and assuming scattering is from an underdense population of N_2^+, the resulting ambipolar diffusion coefficient altitude profile would appear as shown in Fig. 6 (summer: upper panel; winter: lower panel). It is not the purpose of this paper to present results from meteor radars; however, the similarity between Fig. 6 and occasional measured profiles of D_a (e.g. Tsutsumi et al., 1994, Fig. 2) is striking.

3 Discussion

Ambipolar diffusion coefficients deduced from fading times of radar echoes from meteor trails are used to determine neutral air temperatures in the upper mesosphere and lower thermosphere. As stated in the Introduction, (also see Tsutsumi, 1999), when the meteor trail plasma frequency is less than the radio frequency, the meteor echoes are referred to as "underdense". In the other case, when the meteor trail plasma frequency is greater than the radio frequency, yielding overdense echoes, the radio wave is reflected from the outside surface of the meteor trail. In the underdense case, the radio wave penetrates into the trail, and it is this case that is considered in this paper, since meteor radar observations derive wind and diffusion estimates from these echoes only. The line electron densities along meteor trail segments of a Fresnel zone diameter length determine the backscattered power (Tsutsumi, 1999). However, the expansion of the meteor trail leads to decreased coherency in the echoes from scatterers within it, thus causing the received signal to fade. Initially, this expansion will be due to molecular diffusion, and gradually the contribution from turbulence, starting at the smallest scales within the viscous-dissipative subrange of the Kolmogorov spectrum (e.g. Hinze, 1975) will increase. The time scales modelled here correspond to the Kolmogorov microscale η (Kolmogorov, 1941), at which, one could roughly say that turbulent eddies are allowed to complete, since inertia overcomes viscous drag (although this visualisation is perhaps better suited to the inner scale = 7.4η; Blix et al., 1990) At longer time scales, and, therefore, at scales within the inertial subrange (Obukov, 1941), the ionisation structure within the trail is quickly destroyed; however, after this time delay, the backscattered power has become so weak that it does not feature in the determination of the characteristic fading time. It should also be stressed that the turbulent contribution to the dissipation of the ionisation structure is indeed just that: a contribution, an enhancement. We are not attempting to hypothesize that turbulence takes the role of the dissipation mechanism, at least not within the time scale of the experiment's determination of echo fading time. If we were to consider overdense echoes, then we would be interested in how diffusion processes increase the meteor trail's diameter (in such a case, the Doppler shift of the echo reflects the expansion rate of the trail, not the background wind in which the trail is embedded). Furthermore, turbulence would corrugate the trail's surface further affecting its radio cross section, and indeed, time scales would be required that allowed for turbulent structures to form of sizes comparable to half the radar wavelength. Nevertheless, for the time scales corresponding to the Kolmogorov microscale, and typical 3 m/s fluctuation (turbulent) velocities, such as those obtained experimentally from Svalbard (80° N) at 85 km altitude by Hall and Röttger (2001), and for other locations (Hocking, 1988), only 1.6 s will be required to achieve a perturbation the same size as the half-wavelength of a 30 MHz radar. As we see from Figs. 4 and 5, in summer, after 1.6 s, the 85 km and lower echoes are still expected to have significant power, assuming only molecular diffusion. A fluctuation velocity of 2–3 m/s, as stated above, is typical, and in reality greater values may occur. It should not be forgotten, moreover, that the numbers obtained above are for a 30 MHz (VHF) radar, and the case will be radically different for a 3 Mhz (MF) system. MF radars are commonly known as "partial reflection radars", obtaining backscatter from structures in refractive index with spatial extent corresponding to a Fresnel zone. VHF systems, on the other hand, are often used for studies of turbulence in which backscatter comes from "eddies" meeting the Bragg condition.

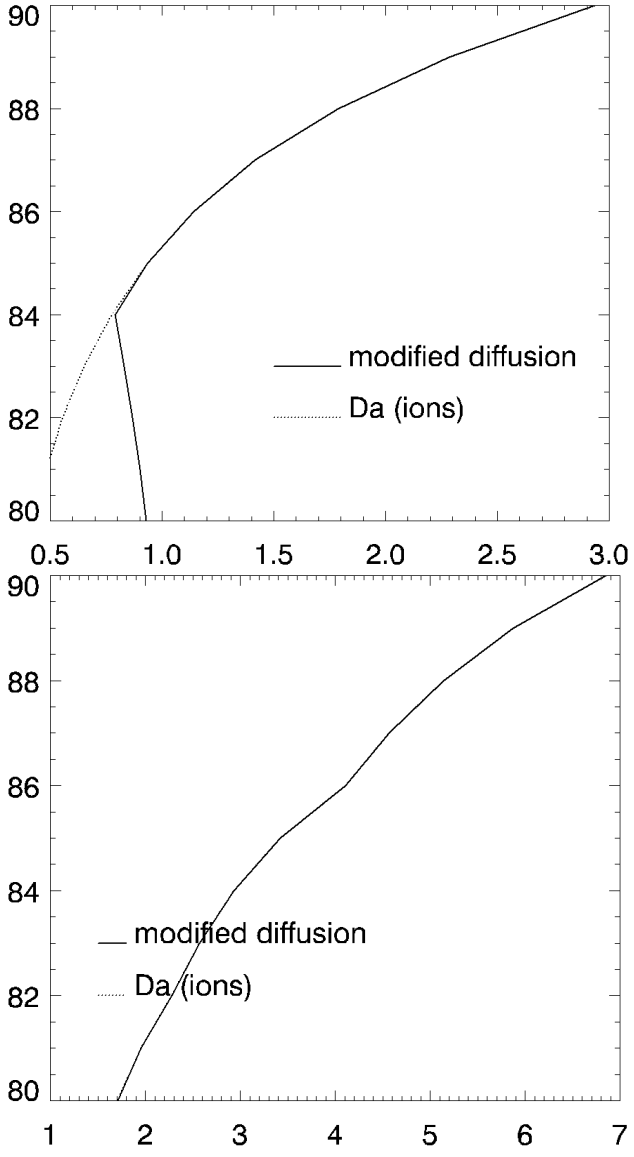

Fig. 6. Simulated profiles of ambipolar diffusion coefficient as might be estimated by a 31 MHz radar situated at 80° N in which the meteor trail ions are assumed to be N_2^+. Upper panel: summer; note the incorrect result below 84 km. Lower panel: winter; turbulence is less of a problem.

To summarize, therefore, this study examines the derivation of the ambipolar diffusion coefficient, combining not

only kinetic theory of ionized gas and radar science, but also fluid dynamics. It has been shown that it is conceivable that neutral air turbulence may accelerate meteor trail dissipation and, therefore, give rise to an overestimation of ambipolar diffusivity. The effect is seasonally dependent due to the variation in temperature profile and the interlinked turbulent energy dissipation. The effect is also a function of radar wavelength and can easily be more acute at lower radar frequencies. The assumptions and analysis method inherent in the derivation of ambipolar diffusivity from the shape of the temporal evolution of the radar echo will, in part, determine the degree to which turbulence affects the results. The temporal and spatial distributions of the turbulence itself are deciding factors, these varying with season and geographical location. If the time resolution of the radar experiment (i.e. averaging time) is comparable to the time scales of intermittency of the turbulence, then temperature fluctuations derived from the radar observations will possibly be misleading.

The simulations presented here may easily be reproduced for specific radar frequencies and at specific geographic locations, to determine whether a given radar may be prone to delivering anomalous echoes.

Acknowledgements. The author thanks W. K. Hocking for advice and the referees for their comments.

Topical Editor D. Murtagh thanks two referees for their help in evaluating this paper.

References

Aso, T., Tsutsumi, M., and Hall, C. M.: First results of NSMR – Nippon/Norway Svalbard Meteor Radar-observations in Longyearbyen in early 2001, Ann. Geophysicae, (submitted), 2001.

Batchelor, G. K.: An Introduction To Fluid Dynamics, pp. 615, Cambridge University Press, 1970.

Blix, T. A., Thrane, E. V., and Andreassen, Ø.: In situ measurements of the fine-scale structure and turbulence in the mesosphere and lower thermosphere by means of electrostatic positive ion probes, J. Geophys. Res., 95, 5533–5548, 1990.

Chilson, P. B., Czechowsky, P., and Schmidt, G.: A comparison of ambipolar diffusion coefficients in meteor trains using VHF radar and UV lidar, Geophys. Res. Lett., 23, 2745–2748, 1996.

Danilov A. D. and Kalgin, Y. A.: Eddy diffusion studies in the lower thermosphere. Adv. Space Res., 17, (11), 17–24, 1996.

Dyrud, L. P., Oppenheim, M. M., and vom Endt, A. F.: The anomalous diffusion of meteor trails, Geophys. Res. Lett., 28, 2775–2778, 2001.

Hall, C. M. and Röttger, J.: Initial observations of Polar Mesospheric Summer Echoes using the EISCAT Svalbard Radar, Geophys. Res. Lett., 28, 131–134, 2001.

Hall, C. M., Brekke, A., Martynenko, O. V., and Namgaladze, A. A.: Turbulent energy dissipation in the high-latitude mesosphere: The PGI97 model, J. Atmos Solar Terr. Phys., 60, 331–336, 1998.

Hedin, A. E.: Extension of the MSIS thermosphere model into the middle and lower atmosphere, J. Geophys. Res., 96, 1159–1172, 1991.

Hinze, J.: Turbulence, pp. 790, McGraw-Hill, 1975.

Hocking, W. K.: Two years of continuous measurements of turbulence parameters in the upper mesosphere and lower thermosphere made with 2-MHz radar, J. Geophys. Res., 93, 2475–2491, 1988.

Hocking, W. K.: Temperatures using radar-meteor decay times, Geophys. Res. Lett., 26, 3297–3300, 1999.

Jones, W.: The decay of radar echoes from meteors with particular reference to their use in the determination of temperature-fluctuations near the mesopause, Ann. Geophysicae, 13, 1104–1106, 1995.

Kolmogorov, A.: The local structure of turbulence in incompressible viscous fluid for very large Reynolds' numbers, C. R. Acad. Sci., 30, 301–305, 1941.

Kundu, P. K.: Fluid Dynamics, pp. 638, Academic Press, 1990.

McDaniel, E. W. and Mason, E. A.: The Mobility and Diffusion of Ions in Gases, John Wiley and Sons, New York, 1973.

McKinley, D. W. R.: Meteor Science and Engineering, pp. 309, McGraw-Hill, 1961.

Obukov, A. M.: On the distribution of energy in the spectrum of turbulent flow, C. R. Acad. Sci., 32, 19–21, 1941.

Shimazaki, T.: Effective eddy diffusion coefficient and atmospheric composition in the lower thermosphere, J. Atmos. Terr. Phys, 33, 1383–1401, 1971.

Tennekes, H. and Lumley, J. L.: A First Course in Turbulence, pp. 300, MIT, USA., 1972.

Tsutsumi, M., Holdsworth, D., Nakamura, T., and Reid, I.: Meteor observations with an MF radar, Earth, Planets Space, 51, 691–699, 1999.

Tsutsumi, M., Tsuda, T., Nakamura, T., and Fukao, S.: Temperature fluctuations near the mesopause inferred from meteor observations with the middle and upper atmosphere radar, Radio Sci., 29, 599–610, 1994.

Weinstock, J.: Vertical turbulent diffusion in a stably stratified fluid, J. Atmos. Sci., 35, 1022–1027, 1978.